



# Olfactory Bulb MRI and Paranasal Sinus CT Findings in Persistent COVID-19 Anosmia

Sedat Giray Kandemirli, MD, Aytug Altundag, MD, Duzgun Yildirim, MD, Deniz Esin Tekcan Sanli, MD, Ozlem Saatci, MD

**Background and purpose:** There is limited literature consisting of case reports or series on olfactory bulb imaging in COVID-19 olfactory dysfunction. An imaging study with objective clinical correlation is needed in COVID-19 anosmia in order to better understand underlying pathogenesis.

**Material and methods:** We evaluated 23 patients with persistent COVID-19 olfactory dysfunction. Patients included in this study had a minimum 1-month duration between onset of olfactory dysfunction and evaluation. Olfactory functions were evaluated with Sniffin' Sticks Test. Paranasal sinus CTs and MRI dedicated to olfactory nerves were acquired. On MRI, quantitative measurements of olfactory bulb volumes and olfactory sulcus depth and qualitative assessment of olfactory bulb morphology, signal intensity, and olfactory nerve filia architecture were performed.

**Results:** All patients were anosmic at the time of imaging based on olfactory test results. On CT, Olfactory cleft opacification was seen in 73.9% of cases with a mid and posterior segment dominance. 43.5% of cases had below normal olfactory bulb volumes and 60.9% of cases had shallow olfactory sulci. Of all, 54.2% of cases had changes in normal inverted J shape of the bulb. 91.3% of cases had abnormality in olfactory bulb signal intensity in the forms of diffusely increased signal intensity, scattered hyperintense foci or microhemorrhages. Evident clumping of olfactory filia was seen in 34.8% of cases and thinning with scarcity of filia in 17.4%. Primary olfactory cortical signal abnormality was seen in 21.7% of cases.

**Conclusion:** Our findings indicate olfactory cleft and olfactory bulb abnormalities are seen in COVID-19 anosmia. There was a relatively high percentage of olfactory bulb degeneration. Further longitudinal imaging studies could shed light on the mechanism of olfactory neuronal pathway injury in COVID-19 anosmia.

**Key Words:** COVID-19; Anosmia; Olfactory bulb; Olfactory nerve; MRI; Olfactory cleft; Paranasal sinus CT.

© 2020 The Association of University Radiologists. Published by Elsevier Inc. All rights reserved.

## INTRODUCTION

COVID-19 related olfactory dysfunction as an isolated symptom or in conjunction with other respiratory symptoms has been increasingly recognized (1). A recent meta-analysis identified 45% of COVID-19 patients had olfactory dysfunction (2). The olfactory dysfunction is sudden onset in majority of cases and is usually a transient entity with a median time to recovery ranging between

1 and 3 weeks (3). No significant association with sinonasal symptoms had been identified, suggesting that pathogenesis of COVID-19 anosmia might differ from obstructive olfactory dysfunction seen in other viral upper respiratory tract infections (1,4). The pathogenesis of COVID-19 anosmia has not been fully defined, however plausible mechanisms are olfactory cleft inflammation/obstruction and/or olfactory bulb damage (1,4).

Magnetic resonance imaging (MRI) dedicated to olfactory nerves is a useful anatomical imaging modality for evaluation of olfactory dysfunction related to postviral infection, trauma, and neurodegenerative processes (5,6). A dedicated MRI study allows assessment of olfactory bulb volume, morphology and signal intensity, status of olfactory nerve filia, and signal intensity of primary olfactory cortex, which is helpful to differentiate between different etiologies and predict prognosis of olfactory function recovery (5).

There is limited literature consisting of case reports on olfactory bulb imaging in COVID-19 olfactory dysfunction. Reported findings included enlarged olfactory bulbs with

### Acad Radiol 2021; 28:28–35

From the University of Iowa Hospital and Clinics, Department of Radiology, Iowa City, Iowa (S.G.K.); Biruni University, Medical Faculty; Acibadem Taksim Hospital, Department of Otolaryngology, Istanbul, Turkey (A.A.); Mehmet Ali Aydinlar University, Acibadem Taksim Hospital, Department of Radiology, Istanbul, Turkey (D.Y.); Acibadem Kozyataği Hospital, Department of Radiology, Istanbul, Turkey (D.E.T.S.); Sancaktepe Training and Research Hospital, Department of Otolaryngology, Istanbul, Turkey (O.S.). Received September 14, 2020; revised October 14, 2020; accepted October 14, 2020. **Address correspondence to:** S.G.K. e-mail: [sedat-kandemirli@uiowa.edu](mailto:sedat-kandemirli@uiowa.edu)

© 2020 The Association of University Radiologists. Published by Elsevier Inc. All rights reserved.

<https://doi.org/10.1016/j.acra.2020.10.006>

internal signal abnormality, olfactory bulb microhemorrhage/enhancement and essentially normal olfactory bulb signal intensity (7–10). However, in majority of the cases, images were not part of an MRI dedicated to olfactory nerves which limit reliability of the findings. Additionally, temporal course and objective assessment of the olfactory dysfunction was lacking in majority of the reports.

A systematic imaging study with objective clinical correlation is needed in COVID-19 anosmia in order to better understand the underlying pathogenesis. In this study, we evaluated a group of patients presenting with persistent COVID-19 related anosmia/hyposmia despite resolution of other COVID-19 related symptoms. Patients were evaluated with objective olfactory tests, paranasal sinus CT, and MRI dedicated to olfactory nerves. We assessed the olfactory cleft opacification; olfactory bulb volume, morphology, and signal intensity; olfactory nerve filia architecture and primary olfactory cortex signal abnormalities.

## MATERIAL AND METHOD

### Patient Selection

This was a prospective study including consecutive patients presenting to a dedicated Smell and Taste Center Clinic with persistent COVID-19 related olfactory dysfunction between May and June 2020. Patients had persistent stable or mildly improved olfactory dysfunction after resolution/recovery of other COVID-19 related symptoms. COVID-19 infection at the time of initial symptoms was confirmed by polymerase chain reaction (PCR) with a swab test. Patients included in this study had a minimum 1-month duration between onset of olfactory dysfunction and evaluation at our center after symptom onset with a range of 1–4 months.

Pediatric and pregnant patients, patients with history of head trauma, preexisting smell and taste alterations, allergic rhinitis and chronic rhinosinusitis were excluded. Institutional review board approval and informed consent were obtained.

### Clinical and Olfactory Function Evaluation

Medical history with a specific focus on olfactory dysfunction for its onset and course, sinonasal symptoms (nasal congestion, rhinorrhea) were obtained. Patients underwent detailed examination of the nose and olfactory region. Olfactory functions were evaluated with Sniffin' Sticks Test battery (Burghart Messtechnik, Germany), which has three components to assess olfactory threshold (T), discrimination (D) and identification (I). Each component has a scale of 1–16, and TDI is a composite score representing the sum of these 3 scores. Normosmia is defined for scores  $\geq 30.5$ , hyposmia for scores between 16.5 and 30.5, and anosmia for scores  $< 16.5$  (11).

### Paranasal Sinus CT

High-resolution paranasal sinus CTs (128 × 2-slice dual-source CT scanner, Siemens, Flash Definition, Erlangen,

Germany) were acquired to assess cribriform plates for evidence of any prior trauma and nasal passage for obstructive causes. Additional reformatted images of olfactory cleft were created with small field of view with 0.4 mm section-thickness and 0.1 mm increment. Olfactory cleft aeration pattern was grouped as normal, partial or total opacification.

### MRI Acquisition

MRI dedicated to olfactory nerves was acquired with a 3 Tesla MRI unit (3 Tesla Magnetom MRI unit, Siemens, Erlangen, Germany) using a 32-channel head coil. Ultra-high resolution T2-space sagittal images (repetition time (TR): 1000 ms, echo time (TE): 136 ms, flip angle: 110°, slice-thickness: 0.6 mm, slice oversampling: 0%, FOV: 200 × 200 mm, matrix: 320 × 320, phase oversampling: 30%, band width: 150 Hz/pixel, voxel size: 0.3 × 0.3 × 1 mm<sup>3</sup>, time of acquisition: 6.08 minutes, echo-train duration: 440 ms) and coronal T2 images covering anterior pole of the olfactory bulb to the primary olfactory region (TR: 6550 ms, TE: 99 ms, flip angle: 150°, slice-thickness: 1 mm, distance factor: 0, FOV: 100 × 100 mm<sup>2</sup>, matrix: 269 × 384, phase oversampling: 56%, bandwidth: 289 Hz/pixel, voxel size: 0.6 × 0.6 × 0.6 mm<sup>3</sup>, time of acquisition: 8.19 minutes, turbo factor: 17) were acquired. Additional conventional sequences for whole brain were obtained.

### MRI Evaluation

Olfactory bulb volume was calculated based on sum of sequential region of interest on consecutive slices using MPR with Syngo.Via Software (VB10B, Siemens). For olfactory volume, cut-off value of 58 mm<sup>3</sup> were used as minimal-normal OB volume as described by Buschhüter et al. (12).

Olfactory sulcus depth was measured on coronal T2 images, by drawing a line tangent to the inferior borders of gyrus rectus and medial orbital gyrus and measuring the depth to the deepest point of the olfactory sulcus (5).

Olfactory bulb morphology was evaluated on high-resolution coronal T2 sections. Oval or inverted-J shape of olfactory bulbs was considered as normal (Fig 1a). Multiple areas ( $\geq 2$ ) of olfactory bulb contour lobulation, rectangular shape or atrophic appearance were considered as abnormal (Fig 1b). Olfactory bulb signal intensity was assessed with contralateral gyrus rectus taken as the reference point. Hyperintense signal abnormality was assessed for its morphology either as diffuse or punctate focus (Figs. 2, 3). A single focus of abnormal signal was not considered as abnormal as bulb region is prone to artifacts (13,14). Images were also reviewed for presence of punctate hypointense regions in the olfactory bulb suggestive of microhemorrhages (Fig 4) (7). Primary olfactory cortex and visualized olfactory tracts were evaluated for presence of abnormal signal intensity on T2 and FLAIR images.

Olfactory nerve filiae were assessed on sagittal T2-space images through the medial and lateral aspects of the bulb. Fine architecture of the filia with uniform distribution at

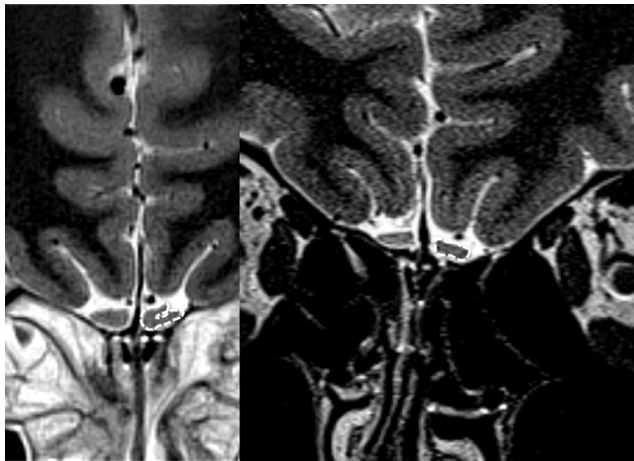


**Figure 1.** (a) Normal J-shaped configuration of the olfactory bulb can be seen on the left side (delineated with dashed arrows) in a normal 20-year-old-female patient with no olfactory dysfunction. (b) An 18-year-old female patient with COVID-19 anosmia rectangular deformation of the olfactory morphology (delineated with dashed arrows).

regular intervals was considered as normal (Fig 5). Regions of focal thickening with nonuniform distribution (clumping) and thinning with scarcity of filia were considered as abnormal (Fig 6).

A single radiologist (D.Y.) with 17 years of experience in head and neck radiology performed the volumetric analysis. Two radiologists (D.Y. and S.G.K. (prior fellowship training in neuroradiology) assessed the olfactory bulb morphology, signal intensity and olfactory nerve filia architecture individually, and reached a consensus for discrepancies.

**Statistical analysis:** All statistical analysis was performed with IBM SPSS Version 21.0 (IBM Corp., Armonk, NY). Descriptive statistics were expressed as number and percentages for categorical variables; and as median and interquartile range for continuous variables. Mann-Whitney *U* test was

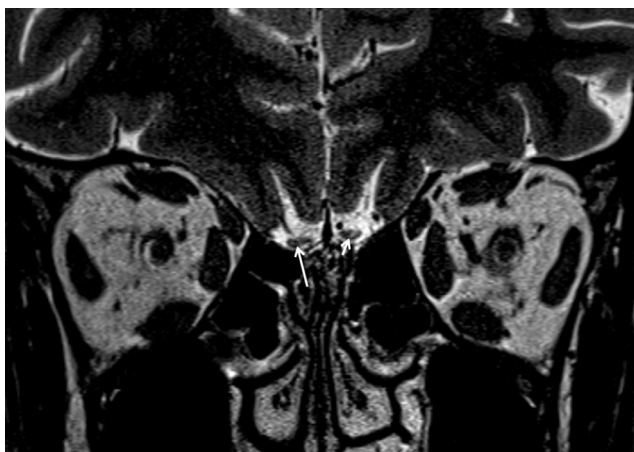


**Figure 2.** A 52-year-old male patient with COVID-19 anosmia. Foci of hyperintensity is noted in the lateral part of right olfactory bulb (long arrow) and dorsolateral part of left olfactory bulb (short arrow) are noted.

used when patients were grouped based on olfactory volume. Spearman test was used for correlation analysis between TDI scores and imaging features. *p* Value <0.05 was considered as statistically significant.

## RESULTS

A total of 23 patients presenting with persistent COVID-19 related olfactory dysfunction were included in the study. Median age was 29 years (interquartile range 22–41) with a slight female predominance ( $n = 14$ , 60.9%). Four patients had sudden onset, isolated olfactory dysfunction; 12 patients with initial olfactory dysfunction followed by COVID-19 related symptoms and 7 patients developed olfactory dysfunction through the course of COVID-19 infection (Flowchart). Seven patients had sinonasal symptoms in the form of rhinorrhea and/or nasal obstruction; remaining 16 patients did not report sinonasal symptoms. Information on demographics, clinical and olfactory symptoms are presented in Table 1. Interval between onset of olfactory dysfunction and evaluation at our center ranged between 1 and 4 months.

At the time of evaluation at Smell and Taste center, all 23 patients were anosmic based on TDI scores. Median threshold score was 1 (interquartile range 1–2.25), median discrimination score was 2 (interquartile range 0–3), median identification score was 2 (interquartile range 0–4), and median TDI score was 4 (interquartile range 1–8.5). Information on TDI scores is presented in Table 1.

### Olfactory Clefts

On paranasal sinus CT, none of the cases had opacification of ethmoid air cells or nasal cavities. Olfactory clefts showed normal aeration in 6 cases, partial opacification in 16 cases and were totally opacified in a single case (Table 2).

### Volume/Sulcus Depth

Median olfactory bulb volume was 62 mm<sup>3</sup> (interquartile range 50.1–66.2 mm<sup>3</sup>) on the right and 60.8 mm<sup>3</sup> (interquartile range 47.4–67.8 mm<sup>3</sup>) on the left (Table 2). Based on the cut-off value of 58 mm<sup>3</sup> described by Buschhüter et al.; olfactory bulb volumes were below normal in 10 cases (12). There was no significant difference between the TDI scores based on cut-off value of 58 mm<sup>3</sup> for bulb volume ( $p = 0.180$ ).

Median olfactory sulcus depths were 6.8 mm (interquartile range 5.4–8.1 mm) on the right and 6.3 mm (interquartile range 4.6–7.6 mm) on the left. Based on a cut-off value of 7.5 mm (48), 14 cases had shallow olfactory sulci. There was a significant negative correlation between total TDI scores and right olfactory sulcus depth ( $r = -0.567$ ,  $p = 0.006$ ). No significant correlation between TDI scores and left olfactory sulcus depths were found. There was no significant correlation between sulcus depth and olfactory bulb volumes ( $p > 0.05$ ).

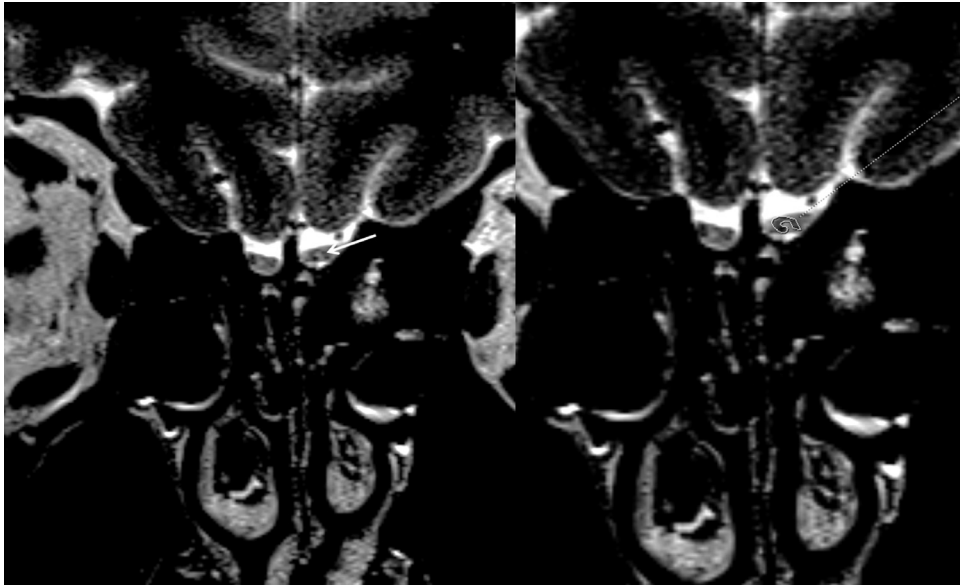


**Figure 3.** A 22-year-old male patient with COVID-19 anosmia. Coronal T2-WI shows increased signal intensity in bilateral olfactory bulbs (arrow depicting the left sided signal abnormality). There is also surrounding incomplete hypointense halo surrounding the left sided signal abnormality (delineated on b).

### Morphology

Morphological classification of the olfactory bulbs and olfactory nerves for groups are presented in [Table 2](#). Type J morphology (usual anatomical shape) was seen in 8 cases (34.8%). Mild contour irregularity with general preservation of J shape was seen in two cases. There was deformed J shape in five cases with rectangular morphology in eight cases.

### Signal Intensity

Olfactory bulb signal intensity was normal in two cases. Diffusely increased signal intensity of the olfactory bulbs was

seen in nine cases, and in seven of these cases this increased signal extended to involve the olfactory tract ([Fig 7](#)).

In 16 cases, there were multiple ( $\geq 2$ ) hyperintense foci in olfactory bulbs. In five of these cases, there was a hypointense halo around the hyperintense foci. Scattered hypointense foci suggestive of microhemorrhages were noted in an additional four cases ([Table 2](#)). No significant differences in TDI scores, olfactory bulb volumes and olfactory sulcus depths were found when MRI findings were grouped based on bulb signal or shape pattern ( $p > 0.05$ ).

Olfactory nerve filia architecture was grossly normal in 13 cases. There was evident clumping in eight cases. There was thinning and scarcity in two cases ([Table 2](#)). No significant differences in TDI scores, olfactory bulb volumes and

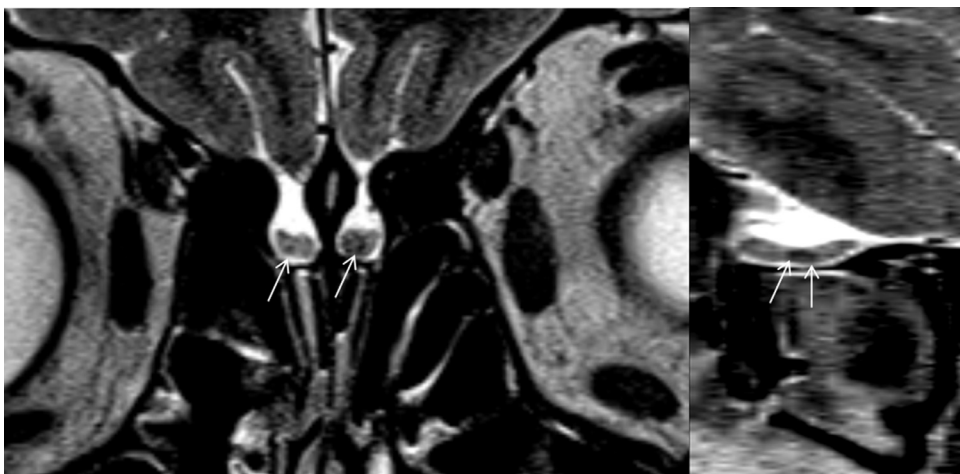


**Figure 4.** A 30-year-old female patient with COVID-19 anosmia. Coronal T2-WI (a) show scattered foci of hypointensities. Sagittal image (b) better demonstrates the extent of the hypointense focus, consistent with microhemorrhages.

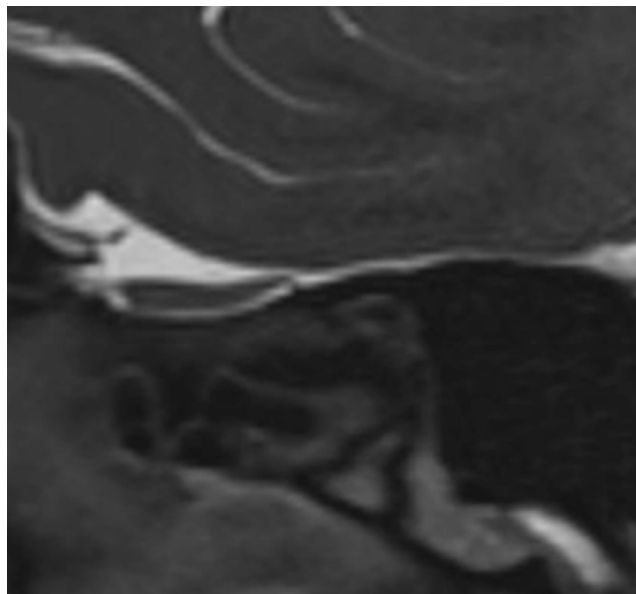


**Figure 5.** Representative image of a normal olfactory bulb on a sagittal T2 space image. Note the biconvex contours and regular signal intensity. The olfactory nerve filia are barely discernible with no clumping or replacement along the inferior margin by CSF signal intensity regions.

olfactory sulcus depths were found when MRI findings were grouped based on filia architecture pattern ( $p > 0.05$ ).

In five cases, there was increased cortical signal intensity in the primary olfactory cortex (Fig 7b).

## DISCUSSION

In this study, we evaluated 23 patients with persistent COVID-19 olfactory dysfunction. All patients were anosmic at the time of imaging based on TDI scores. We noted a high

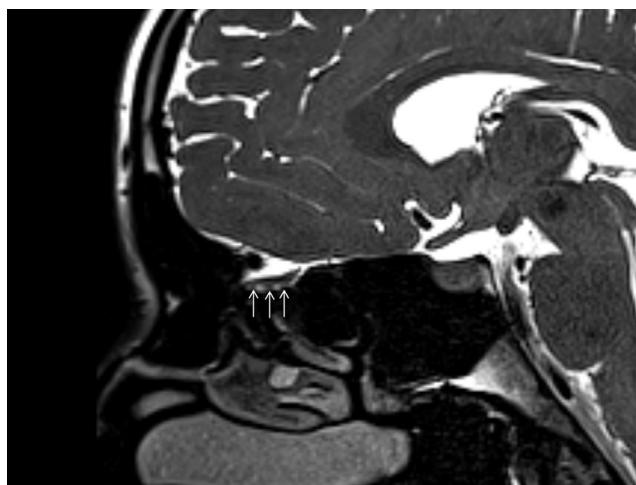


**Figure 6.** A 30-year-old male patient with COVID-19 anosmia. Sagittal T2-WI shows thickening and clumped appearance of the olfactory nerve filia (arrow).

**TABLE 1. Demographic and Clinical Features of Persistent COVID-19 Anosmia Cases**

Total number of cases	23
Age*	29 (22–41) years
Sex	14 female, 9 male
<i>Onset of COVID-19 anosmia</i>	
Sudden, isolated	4 (17.4%)
Initial anosmia, subsequent other COVID-19 symptoms	12 (52.2%)
Initial other COVID-19 symptoms with onset of anosmia	7 (30.4%)
<i>Sinonasal symptoms at anosmia onset</i>	7 (30.4%)
<i>Interval between anosmia onset and MRI*</i>	1–4 months
<i>Sniffin' Sticks test</i>	
Threshold (T)*	1 (1–2.25)
Discrimination (D)*	2 (0–3)
Identification (I)*	3 (0–4)
TDI*	4 (1–8.5)

Data is presented as median and interquartile range.

percentage of olfactory cleft opacification (73.9% of cases). There was reduction of olfactory bulb volumes, change in bulb shape and signal abnormalities. Some of the cases showed olfactory nerve filia clumping or scarcity. Additionally, 21.7% of cases had primary olfactory cortical signal abnormality.

Pathogenesis of olfactory dysfunction in COVID-19 disease is still incompletely understood, but there are some distinct features that separate this entity from other postviral olfactory dysfunction. Postviral anosmia in the setting of upper respiratory tract infection can account up to 40% of the cases, and is usually related to mucosal congestion and nasal obstruction (15). This can affect the airflow and impair the travel of odorants, despite an intact olfactory epithelium, and result in a conductive olfactory loss (4). On the other hand, there is no significant association with sinonasal symptoms in COVID-19 anosmia, as also shown in our cohort (16). This suggests that mechanisms other than sinonasal obstruction may play a role. Plausible mechanisms include direct damage to olfactory epithelium and olfactory bulb by the virus, and damage to olfactory epithelium secondary to inflammatory changes (4).

Angiotensin converting enzyme 2 (ACE2) receptors, which are the target molecules for SARS-CoV-2, are expressed by non-neuronal supporting cells of the olfactory epithelium, but not directly by the olfactory neurons, which might be the putative target site for the virus (4,17). Part of the olfactory dysfunction can be due to injury to supporting cells of the olfactory epithelium. This is supported by postviral anosmia studies where persistence of olfactory dysfunction weeks to months after resolution of rhinitis reflects the interval for olfactory epithelium regeneration (4). Pathological studies in postviral anosmia studies have shown absence of cilia and reduced

**TABLE 2. Olfactory Cleft Opacification, Bulb Morphology, Signal Changes, Olfactory Nerve Filia Morphology, and Primary Olfactory Cortex Findings in Persistent COVID-19 Anosmia**

	n = 23
<i>Olfactory cleft opacification</i>	17 (73.9%)
Partial	16 (69.6%)
Total	1 (4.3%)
<i>Olfactory bulb morphology</i>	
Normal	8 (34.8%)
Mild irregularity with preserved J shape	2 (8.7%)
Contour lobulations	5 (21.7%)
Rectangular shape	8 (34.8%)
<i>Olfactory bulb signal abnormalities</i>	
Normal	2 (8.7%)
Diffusely increased signal	9 (39.1%)
Hyperintense foci	16 (69.6%)
Hyperintense foci with halo	5 (21.7%)
Microhemorrhages	4 (17.4%)
<i>Olfactory tract signal abnormality</i>	7 (30.4%)
<i>Olfactory cortex signal abnormality</i>	5 (21.7%)
<i>Olfactory nerve morphology</i>	
Grossly normal	13 (56.5%)
Evident Clumping	8 (30.4%)
Thinning with scarcity	2 (8.7%)
	<i>Olfactory bulb volume, mm<sup>3</sup></i>
Right	62 (50.1–66.2)
Left	60.8 (47.4–67.8)
	<i>Olfactory sulcus depth, mm</i>
Right	6.8 (5.4–8.1)
Left	6.3 (4.6–7.6)

Olfactory bulb volumes and olfactory sulcus depths in persistent COVID-19 anosmia.

number of olfactory sensory neurons replaced by metaplastic squamous epithelium (18,19). COVID-19 patients with slow recovery of olfactory function might have a greater extent of

intranasal injury. Another potential mechanism is direct damage to olfactory nerves and retrograde invasion of olfactory tracts (4). Neurotropic potential of coronaviruses has been demonstrated, however absence of ACE2 receptors in olfactory neurons does not support this hypothesis (17). The best example of retrograde olfactory neuroinvasion with anosmia is described in herpes simplex virus. Histological analysis of olfactory epithelium in herpes simplex encephalitis patients has shown diffuse inflammation and ragged appearance of the cells with hemorrhage along perineural sheaths (20). However, pathological evidence for olfactory nerve invasion in COVID-19 is not available currently.

### Olfactory Clefts

Olfactory clefts are lined by olfactory epithelium which also contain the olfactory receptor neurons (21). Axons of these neurons cross the cribriform plate as olfactory filia and synapse in the olfactory bulbs. Various sinonasal pathologies can cause mucosal inflammation and obstruction in lower parts of the nasal cavities, resulting in blockage of odors to reach the olfactory cleft (16). In our series, none of the cases had mucosal synechia in the nasal cavities.

As described previously, there can be secondary inflammatory changes in olfactory clefts due to viral invasion which could result in mucosa edema with subsequent narrowing of the olfactory cleft. In our study, we identified partial and total olfactory cleft opacification in 69.6% and 4.3% of cases, respectively, supporting this hypothesis. Review of the available paranasal sinus CT literature on COVID-19 anosmia shows that majority of patients did not have significant pathological changes with partial opacification of the olfactory cleft noted in some cases (22).

### Olfactory Bulb Imaging

MRI of olfactory nerves provides useful anatomical details for evaluation of olfactory bulb, olfactory nerve filia and primary

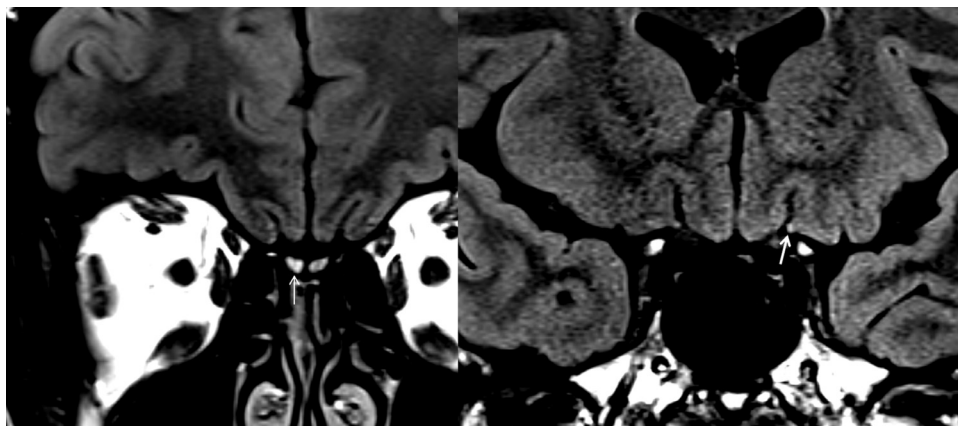


**Figure 7.** A 37-year-old female patient with COVID-19 anosmia. Coronal 3D FLAIR image (a) shows diffuse increased in bilateral olfactory bulbs (more prominent on the right side, marked with arrow). More posterior coronal FLAIR image (b) at the level of olfactory stria shows subtle increased cortical signal intensity at primary olfactory cortex (arrow).

olfactory cortex in patients with anosmia. Majority of the literature on postviral anosmia evaluated the olfactory bulb volume, which showed correlation with olfactory function (23,24). Olfactory bulb can also be assessed for its overall morphology, where loss of oval or inverted J shape is suggestive of abnormal structure (23). Additionally, olfactory bulb can be assessed for presence of signal abnormalities in the form of hyperintensities indicating degeneration and hypointensities representing microhemorrhages (7). Olfactory nerve filia can be assessed for clumping or scarcity, which suggests inflammatory changes and degenerative/traumatic loss, respectively.

Literature on olfactory bulb imaging in COVID-19 anosmia is limited, derived from conventional brain images instead of dedicated sequences. Additionally, there is variability in timing of imaging, and objective assessment of olfactory dysfunction (7–10,25,26). Some of the initial case reports reported normal olfactory bulb volume with normal signal intensity (8,27). Later on, Aragao et al. in a case series demonstrated olfactory bulb abnormality as either microbleeding or abnormal enhancement on MR imaging (7). However, in this study, images were not dedicated to olfactory bulbs. Laurendon et al. demonstrated severe enlargement of the olfactory bulbs with abnormal high signal intensity on T2, consistent with bulb edema in a patient with COVID-19 anosmia (9). The olfactory pathways, including the cortical projections had normal signal intensity. Control imaging when olfactory functions recovered showed normalization of the olfactory bulb imaging findings (9). Li et al. showed decreased right olfactory bulb volume and increased linear hyperintensities in bilateral olfactory bulbs in a COVID-19 anosmia case (26). Politi et al. showed subtle hyperintensity in bilateral olfactory bulbs accompanied by right gyrus rectus hyperintensity in a COVID-19 anosmia case. Control imaging 28-days later (when anosmia had recovered) showed complete resolution of cortical signal abnormality, with decreased volume of the olfactory bulbs with partial resolution of the internal signal abnormality (10). Our study population is different compared to the rest of literature, where we focused on a targeted population of persistent COVID-19 cases, whereas the available literature mainly reports acute findings in temporary anosmia. In this aspect, our findings may reflect changes in cases that had higher degree of olfactory epithelial damage and subsequent olfactory bulb involvement. There was no significant correlation between TDI scores and imaging findings except for olfactory sulcus depths, however considering the fact that majority of cases were anosmic with low TDI score, we may not have detected small differences between groups.

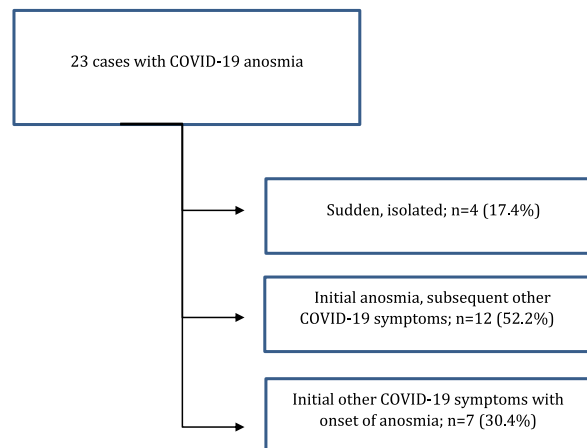
There are some limitations to our study. Main limitation is the relatively low number of patients given the extensive work-up required for inclusion in the study like requirement for completing ENT examination, smell test, and olfactory MRI. There might be a selection bias, as patients with more severe respiratory/systemic COVID-19 infection may not have been included in the study, as these patients more likely have a protracted disease course and did not present to our Smell disorder outpatient clinic. Additionally, we imaged

patients after a median interval of 1–4 months from onset of olfactory dysfunction. So these imaging findings may reflect the subacute and chronic state of changes, rather than the acute changes. Assessment of olfactory bulb and olfactory filia for signal intensity and morphology requires extensive experience with high level of attention to details. Another point to consider is the correlation between neuromalacic hyperintense changes in the olfactory bulbs and olfactory loss is still vague, as neuromalacic signal changes could also be identified in patients with normosmia (23).

## CONCLUSION

This is the first systemic olfactory nerve imaging study with objective olfactory tests available in persistent COVID-19 anosmia. Our findings support the observations of olfactory cleft inflammation in COVID-19 anosmia. Additionally, relatively high percentage of olfactory bulb degeneration suggests that direct/indirect injury to olfactory neuronal pathways also take place, specifically in cases with persistent post COVID-19 anosmia.

### Flowchart



## CONFLICTS OF INTEREST

None to declare.

## FUNDING INFORMATION

None to declare.

## REFERENCES

- Cooper KW, Brann DH, Farruggia MC, et al. COVID-19 and the chemical senses: supporting players take center stage. *Neuron* 2020; 107:219–233.
- Hoang MP, Kanjanaumporn J, Aumjaturapat S, et al. Olfactory and gustatory dysfunctions in COVID-19 patients: a systematic review and meta-analysis. *Asian Pac J Allergy Immunol* 2020; 38:162–169.
- Lee Y, Min P, Lee S, et al. Prevalence and duration of acute loss of smell or taste in COVID-19 patients. *J Korean Med Sci* 2020; 35:e174.
- Han AY, Mukdad L, Long JL, et al. Anosmia in COVID-19: mechanisms and significance. *Chem Senses* 2020.
- Duprez TP, Rombaux P. Imaging the olfactory tract (cranial nerve #1). *Eur J Radiol* 2010; 74:288–298.

6. Rombaux P, Duprez T, Hummel T. Olfactory bulb volume in the clinical assessment of olfactory dysfunction. *Rhinology* 2009; 47:3–9.
7. Aragão M, Leal MC, Cartaxo Filho OQ, et al. Anosmia in COVID-19 associated with injury to the olfactory bulbs evident on MRI. *AJNR Am J Neuroradiol* 2020; 41:1703–1706.
8. Galougahi MK, Ghorbani J, Bakhshayeshkaram M, et al. Olfactory bulb magnetic resonance imaging in SARS-CoV-2-induced anosmia: the first report. *Acad Radiol* 2020; 27:892–893.
9. Lairendon T, Radulesco T, Mugnier J, et al. Bilateral transient olfactory bulbs edema during COVID-19-related anosmia. *Neurology* 2020; 95:224–225.
10. Politi LS, Salsano E, Grimaldi M. Magnetic resonance imaging alteration of the brain in a patient with coronavirus disease 2019 (COVID-19) and anosmia. *JAMA Neurol* 2020; 77:1028–1029.
11. Hummel T, Kobal G, Gudziol H, et al. Normative data for the “Sniffin’ Sticks” including tests of odor identification, odor discrimination, and olfactory thresholds: an upgrade based on a group of more than 3,000 subjects. *Eur Arch Otorhinolaryngol* 2007; 264:237–243.
12. Buschhüter D, Smitka M, Puschmann S, et al. Correlation between olfactory bulb volume and olfactory function. *Neuroimage* 2008; 42:498–502.
13. Tsutsumi S, Ono H, Yasumoto Y. Visualization of the olfactory nerve using constructive interference in steady state magnetic resonance imaging. *Surg Radiol Anat* 2017; 39:315–321.
14. Leboucq N, Menjot de Champfleu N, Menjot de Champfleu S, et al. The olfactory system. *Diagn Interv Imaging* 2013; 94:985–991.
15. Welge-Lüssen A, Wolfensberger M. Olfactory disorders following upper respiratory tract infections. *Adv Otorhinolaryngol* 2006; 63:125–132.
16. Jalessi M, Barati M, Rohani M, et al. Frequency and outcome of olfactory impairment and sinonasal involvement in hospitalized patients with COVID-19. *Neurol Sci* 2020; 1–8.
17. Brann D, Tsukahara T, Weinreb C, et al. Non-neural expression of SARS-CoV-2 entry genes in the olfactory epithelium suggests mechanisms underlying anosmia in COVID-19 patients. *Sci Adv*. 2020; 31:eabc5801. doi:10.1126/sciadv.abc5801.
18. Jafek BW, Hartman D, Eller PM, et al. Postviral olfactory dysfunction. *Am J Rhinol* 1990; 4:91–100.
19. Yamagishi M, Fujiwara M, Nakamura H. Olfactory mucosal findings and clinical course in patients with olfactory disorders following upper respiratory viral infection. *Rhinology* 1994; 32:113–118.
20. Twomey JA, Barker CM, Robinson G, et al. Olfactory mucosa in herpes simplex encephalitis. *J Neurol Neurosurg Psychiatry* 1979; 42:983–987.
21. Trotier D, Bensimon JL, Herman P, et al. Inflammatory obstruction of the olfactory clefts and olfactory loss in humans: a new syndrome? *Chem Senses* 2007; 32:285–292.
22. Naeini AS, Karimi-Galougahi M, Raad N, et al. Paranasal sinuses computed tomography findings in anosmia of COVID-19. *Am J Otolaryngol* 2020; 41:102636.
23. Chung MS, Choi WR, Jeong HY, et al. MR imaging-based evaluations of olfactory bulb atrophy in patients with olfactory dysfunction. *AJNR Am J Neuroradiol* 2018; 39:532–537.
24. Rombaux P, Huart C, Deggouj N, et al. Prognostic value of olfactory bulb volume measurement for recovery in postinfectious and posttraumatic olfactory loss. *Otolaryngol Head Neck Surg* 2012; 147:1136–1141.
25. Eliezer M, Hautefort C. MRI Evaluation of the olfactory clefts in patients with SARS-CoV-2 infection revealed an unexpected mechanism for olfactory function loss. *Acad Radiol* 2020; 27: 1191-1191.
26. Li CW, Syue LS, Tsai YS, et al. Anosmia and olfactory tract neuropathy in a case of COVID-19. *J Microbiol Immun Infect* 2020.
27. Eliezer M, Hautefort C, Hamel A-L, et al. Sudden and complete olfactory loss of function as a possible symptom of COVID-19. *JAMA Otolaryngol Head Neck Surg* 2020; 146:674–675.